Heliyon 10 (2024) e30512

Contents lists available at ScienceDirect

Heliyon

journal homepage: www.cell.com/heliyon

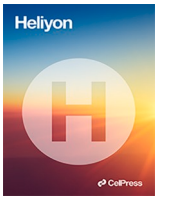

Research article

Subacromial bursa in patients with rotator cuff tear with or without adhesive capsulitis exhibits a differential transcriptome with potential molecular biomarkers☆

Qiuyuan Wang [a], Feng Zhou [a], Pingcheng Xu [a,b], Lingying Zhao [c,d], Jiong Jiong Guo [a,d,e,*]

[a] Department of Orthopedics and Sports Medicine, The First Affiliated Hospital of Soochow University, Suzhou, PR China
[b] Department of Orthopedics, Suzhou Wujiang District Fourth People's Hospital, Suzhou, PR China
[c] Department of Hematology, National Clinical Research Center for Hematologic Disease, The First Affiliated Hospital of Soochow University, Suzhou, PR China
[d] Jiangsu Institute of Hematology, Key Laboratory of Thrombosis and Hemostasis of Ministry of Health of PR China, Suzhou, PR China
[e] China-Europe Sports Medicine Belt-and-Road Joint Laboratory, Ministry of Education of PR China, PR China

ARTICLE INFO

Keywords:
Rotator cuff tear
Adhesive capsulitis
RNA-Seq
Subacromial bursa

ABSTRACT

Background: Although adhesive capsulitis (AC) is a common condition, the pathological mechanisms remain understudied. The purpose of our research was to evaluate variations in gene expression across the entire genome in the subacromial bursa tissue of individuals with rotator cuff tears (RCT), with or without AC, and to explore the factors that may influence the occurrence and progression of AC.

Methods: Transcription profiles of subacromial bursa samples from 12 RCT patients, of whom 6 had also AC, were evaluated. Data were generated using RNA-seq. DESeq2 was utilized to identify the differentially expressed genes (DEGs) in both groups. In order to conduct a more in-depth examination of the DEGs, we performed Gene Ontology (GO) functional enrichment and Kyoto Encyclopedia of Genes and Genomes (KEGG) pathway analysis. A network of interactions between proteins was built, and the central genes were determined using Cytoscape. The hub genes were confirmed through qRT-PCR and immunohistochemistry.

Results: 324 of the 16,251 detected genes were identified as DEGs. Analysis of GO functional enrichment showed that the DEGs were enriched in domains of biological process, molecule function and cellular component. Analysis of KEGG pathways revealed enrichment of DEGs in pathways like IL-17 signaling and ECM-receptor interaction. We verified that the association between AC and the increase in expression of the PPI network hub genes.

Conclusion: This study investigated the transcriptome differences of subacromial bursa in RCT patients with or without AC. Using bioinformatics technology, we identified the DEGs and screened out the hub genes. The research enhanced the data on gene expression profiles of DEGs in the subacromial bursa tissue of patients with RCT, offering fresh perspectives on the regulation of gene transcription.

☆ Dr. Wang and Zhou contributed equally to this article.

* Corresponding author. 188 Shizi Street, Suzhou, 215006, PR China.
E-mail addresses: wangqiuyuan_1999@163.com (Q. Wang), drzhoufeng1991@163.com (F. Zhou), 136645478@qq.com (P. Xu), jssandyzly@163.com (L. Zhao), drjjguo@163.com, guojiongjiong@suda.edu.cn (J.J. Guo).

https://doi.org/10.1016/j.heliyon.2024.e30512
Received 12 January 2024; Received in revised form 23 April 2024; Accepted 29 April 2024
Available online 30 April 2024

1. Background

Rotator cuff tear (RCT) is a common joint disease that causes joint pain and dysfunction. The frequency of RCT rises with advancing age and surpasses 25 % in individuals aged 60 and above [1]. The treatment of RCT through open or arthroscopic surgery has been implemented worldwide for decades, and the overall effect is satisfactory. Up to 10 %–40 % of patients with RCT have a concomitant adhesive capsulitis [2].

Adhesive capsulitis also called as frozen shoulder, is another common disease which affects 2 %–5 % of general population worldwide [3]. Shoulder pain and limited range of motion may result from AC. The fibrosis of the shoulder joint capsule is a characteristic pathological feature of AC. Treatments modalities for AC include medication, local steroid injection, physiotherapy, and even surgical release [4].

However, there is no consensus on treating RCT patients with AC [5]. Repairing the torn cuff surgically involves tightening the joint, potentially worsening stiffness. In addition to surgery, biological technology is also applied to the treatment, such as such as platelet-rich plasma injection [6]. Therefore, it is necessary to further study the pathological changes of RCT and explore new therapeutic targets.

The study of transcriptomics offers a method for examining diseases on a cellular scale, potentially aiding in identifying disease causes. RNA-seq is a crucial tool in transcriptomics research for analyzing gene expression in tissues and cells. RNA-seq analysis of the subacromial bursa in individuals with RCT may provide new perspectives on the pathogenesis and molecular characteristics of these disorders.

This study aimed to analyze variations in gene expression across the entire genome in subacromial bursa tissue of RCT patients with or without AC, while also investigating factors that may influence the development and occurrence of AC.

In our study, RNA-seq was utilized to detect genes that were expressed differently in the subacromial bursa tissue of RCT patients with or without AC. Furthermore, the differentially expressed genes (DEGs) were analyzed using Gene Ontology (GO) functional enrichment and Kyoto Encyclopedia of Genes and Genomes (KEGG) pathway analysis. Next, we built the protein-protein interaction (PPI) networks to identify hub genes. The confirmed hub genes could be utilized as biomarkers to distinguish variations in the subacromial bursa tissues of RCT individuals with or without AC, owing to their pivotal function in gene expression networks.

2. Materials and methods

2.1. Patients and sample collection

From September 2022 to November 2022, patients who had symptomatic RCT and underwent surgery at the First Affiliated Hospital of Soochow University were assessed. Every patient underwent shoulder X-ray (anteroposterior view and supraspinatus-outlet view) and MRI before surgery. By utilizing both imaging and patient history, we ruled out patients with related glenohumeral injuries like Bankart lesions, osteoarthritis alterations, and large rotator cuff tears (tear size $>$ 5 cm). Large aera tears were not considered due to their increased likelihood of functional impairment and may be misinterpreted as AC. To reduce the impact of other variables that are linked to the development of AC, individuals with metabolic conditions like diabetes mellitus and thyroid problems were not included in the study. The study also excluded patients who had previously acute trauma, dislocation, fracture, surgery on the shoulder, and stiffness on both sides. Information on demographics (age, gender, BMI) and disease characteristics, such as duration and range of motion (ROM) of the affected shoulder in various positions, was gathered. AC was defined as limited passive ROM of less than 25 % or 30° in comparison to the standard or opposite side in at least two out of three movements, which including flexion, external rotation at side, and internal rotation at back [7]. The subacromial bursa tissues were carefully examined and excised using arthroscopic techniques during the surgical procedure. Upon collection, the samples were promptly frozen in liquid nitrogen and subsequently kept at −80 °C until needed for future studies. Patient evaluation and surgery were performed by the same senior shoulder surgeon. The authors' organization's institutional review board approved the research procedures. All patients signed a consent form before inclusion.

2.2. RNA isolation and library preparation

Total RNA was extracted from the subacromial bursa tissues using the TRIzol reagent (Invitrogen, CA, USA) according to the manufacturer's protocol. The NanoDrop 2000 Spectrophotometer (Thermo Scientific, USA) was utilized to assess the quality and measure the amount of RNA. RNA quality was evaluated with the Agilent 2100 Bioanalyzer (Agilent, California, USA). Subsequently, the libraries were built with the RNA-seq Library Prep Kit in accordance with the instructions provided by the manufacturer. OE Biotech Co., Ltd. (Shanghai, China) performed the sequencing of the transcriptome.

2.3. RNA sequencing and DEGs analysis

Sequencing of the libraries was performed using the illumina Novaseq 6000 platform and 150 bp paired-end reads were generated. Fastq format raw reads were initially processed with fastp to eliminate low-quality reads and obtain clean reads [8]. The clean reads were aligens to the source genetic material with the assistance of HISAT2 [9]. The FPKM value for every gene was computed and the number of reads for each gene was determined using HTSeq-count [10,11]. Principal component analysis (PCA) was conducted using R Statistical Software (version 3.2.0) to evaluate the biological replication in the samples.

DEGs analysis was performed using the DESeq2 [12]. A threshold was set for genes showing significantly DEGs with an adjusted P value < 0.05 and foldchange >2 or foldchange <0.5.

2.4. GO functional enrichment and KEGG pathway analysis

The DEGs were analyzed for functional enrichment using GO annotations [13], covering biological process (BP), molecular function (MF), and cellular component (CC) domains, as well as KEGG pathway analysis [14]. The KEGG database offers comprehensive data on gene functions, encompassing biochemical pathways and interactions at both the molecular and systemic levels. Gene clusters were annotated and visualized for biological themes using the clusterProfiler package, a tool in R. The hypergeometric test was utilized for conducting enrichment analysis. A threshold of less than 0.05 was selected as the significance level to identify a statistically meaningful difference.

2.5. PPI network and hub gene analysis

The PPI networks were constructed using the STRING database [15]. The minimum interaction score needed had the medium confidence (score >0.4). Cytoscape (version 3.9.0) was used to visualize these PPI networks. We analyzed the primary functional components with the assistance of the Molecular Complex Detection Technology (MCODE) plugin. Scoring each gene node using the MCC algorithm and CytoHubba plugin. The GeneMANIA website [16],which is utilized for building PPI networks, was employed to forecast gene function and identify genes that have similar impacts. GeneMANIA was utilized in the research to discover hub genes' PPI networks.

2.6. Validation of hub gene expression by qRT-PCR

Quantitative real-time PCR (qRT-PCR) was performed to confirm the accuracy of RNA-seq analysis in detecting the DEGs and to assess the expression levels of the hub genes. RNA was isolated from subacromial bursa tissue samples with TRIzol Reagent and converted to cDNA using SweScript All-in-One SuperMix (Thermo Scientific, USA). A qRT-PCR was then performed using the SYBR Green qPCR Master Mix (None ROX, Thermo Scientific, USA). GAPDH gene served as the internal control. The mRNA expression was calculated using the $2^{-\Delta\Delta Ct}$ method. In this method, group C was used as the control group.

2.7. Immunohistochemistry (IHC)

Samples were selected for paraffin embedding and sectioning. The area was marked with hematoxylin-eosin (HE) staining. MMP2, MMP9, COL1A1, and PTGS2 expression (dilution 1:50, Thermo Fisher Scientific) were identified using the immunohistochemistry kit instructions (ZSBIO, China). Briefly, the endogenous peroxidase of sections was inactivated by incubation with 3 % of H2O2 for 10 min. Next, the portions were exposed to thinned antibodies, such as MMP2, MMP9, COL1A1, and PTGS2, overnight at 4 °C. Images were acquired using a slice scanner (Pannoramic MIDI, 3DHISTECH). Positive cells were counted using Image J software (version 1.54). The counts were conducted by two separate observers, and the average value was determined.

2.8. Statistical analysis

Data were expressed as mean ± standard deviation. Differences between two groups were compared via two-sided Student's t-test. Data with $p < 0.05$ were considered to have statistically significant differences. In this study, "*"and "**" denoted $p < 0.05$ and $p < 0.01$, respectively. The data analysis was calculated with SPSS 22.0 analysis software (SPSS Inc, Chicago, IL, USA).

Table 1
Demographic characteristics of the included patients.

Variables		RCT patients with AC (n = 6)	RCT patients without AC (n = 6)	p-value
Age (years)		54.83 ± 7.99	58.50 ± 13.60	0.582*
Gender	Male	2 (33.3 %)	2 (33.3 %)	1**
	Female	4 (66.7 %)	4 (66.7 %)	1**
BMI (kg/m^2)		24.47 ± 6.24	23.58 ± 3.04	0.762*
Disease duration (months)		4.50 ± 1.87	5.50 ± 2.07	0.401*

The data are presented as mean ± standard deviation or frequency (percentage). * obtained from independent-samples *t*-test, ** obtained from Fisher's precision probability test.
Legend: AC = adhesive capsulitis, BMI = body mass index, RCT = rotator cuff tear.

3. Results

3.1. Population characteristics

Twelve patients were included: 6 with RCT and AC (named as group E), 6 with RCT without AC (named as group C). Table 1 contains information on the demographics. There were no statistically significant differences between the two groups. Mean ROM of the enrolled patients are listed in Table 2.

3.2. Identification of the DEGs

Sequencing data comprised 16,251 genes, 324 of them were identified as the DEGs. Among these, 158 genes were upregulated and 166 genes were downregulated. Fig. 1A shows the Principal Component Analysis (PCA) plot of the samples. In Fig. 1B and **C,** the volcano plot and heatmap display the DEGs respectively. Table 3 provides details on the top 30 DEGs. **Additional file 1: Table S1 contains information about all DEGs.**

3.3. GO functional enrichment and the KEGG pathway analysis

Analysis of GO functions showed that the DEGs were enriched in extracellular matrix organization ($P = 4.95 \times 10-11$), collagen catabolic process ($P = 1.89 \times 10-9$), and extracellular matrix disassembly ($P = 1.37 \times 10-6$) functions within the BP domain. In the MF category, the DEGs showed enrichment in metalloendopeptidase activity ($P = 1.93 \times 10-6$), growth factor activity ($P = 9.28 \times 10-5$), and serine-type endopeptidase activity ($P = 9.81 \times 10-5$) functions. Inthe CC category, the DEGs showed enrichment in the extracellular space ($P = 2.10 \times 10-14$), extracellular region ($P = 9.42 \times 10-9$), and extracellular matrix ($P = 3.56 \times 10-8$) functions (Fig. 2A).

In accordance with the functional classification, GO is typically divided into three levels. Level 1 encompasses three entries: BP, CC and MF. Level 2 comprises 64 entries, including cellular process, cell and binding. Level 3 encompasses various entries utilized for conventional enrichment. The functions from level 1 to level 3 are more specific. Fig. 2B shows the comparative distribution of differential genes at GO Level 2.

Analysis of KEGG pathway revealed that the DEGs were concentrated in the IL-17 signaling pathway ($P = 1.25 \times 10-3$), Endocrine resistance ($P = 1.50 \times 10-3$), Parathyroid hormone synthesis, secretion and action ($P = 1.25 \times 10-3$), ECM-receptor interaction ($P = 4.33 \times 10-3$) and other pathways (Fig. 3). The important pathways involved in the IL-17 signaling pathway and ECM-receptor interaction are shown in Fig. 4A and B.

3.4. PPI network construction and identification of hub genes

Our analysis produced 318 nodes and 550 edges using the STRING database. The PPI enrichment *P*-value was $1.0 \times 10-16$.10 modules were discovered using the MCODE extension in Cytoscape. The valuablethree modules are showen in Fig. 5A,B,C,D. Through the utilization of cytoHubba extension in Cytoscape, we finally identified Interleukin 6 (IL6), Matrix Metallopeptidase 1 (MMP1), MMP2, MMP3, MMP9, Collagen Type I Alpha 1 Chain (COL1A1), Periostin (POSTN), RUNX Family Transcription Factor 2 (RUNX2), Twist Family BHLH Transcription Factor 1 (TWIST1), Prostaglandin-Endoperoxide Synthase 2(PTGS2) genes as the hub genes.

Next, we used the GeneMANIA database to investigate the co-expression networks and potential functions of the hub genes (Fig. 6). The intricate PPI networks were unveiled, showcasing genetic interactions at 0.83 %, predicted at 3.52 %, co-localization at 4.69 %, physical interactions at 8.29 %, shared-protein domains at 17.33 %, co-expression at 65.79 %. Analysis of function showed that they are associated with pathways such as collagen metabolic process, metallopeptidase activity, extracellular matrix organization, regulation of inflammatory response, skeletal system development, demonstrating their involvement in disease development.

3.5. Validation of the hub genes and immunohistochemistry

QRT-PCR was used to confirm the levels of expression of the 10 hub genes in the subacromial bursa tissue collected from RCT

Table 2
Mean range of motion of the included patients.

Variables	RCT patients with AC (n = 6)	RCT patients without AC (n = 6)	p-value
Active Flexion ROM (°)	79.17 ± 15.62	103.33 ± 9.83	0.009*
Active Abduction ROM (°)	69.17 ± 9.17	95.00 ± 15.49	0.006*
Active Internal Rotation ROM (°)	24.17 ± 3.76	32.50 ± 10.84	0.106*
Active External Rotation ROM (°)	46.67 ± 9.83	55.83 ± 11.58	0.170*
Passive Flexion ROM (°)	81.67 ± 18.07	102.50 ± 14.40	0.052*
Passive Abduction ROM (°)	70.83 ± 9.17	99.17 ± 15.94	0.004*
Passive Internal Rotation ROM (°)	27.50 ± 4.18	35.00 ± 11.40	0.161*
Passive External Rotation ROM (°)	50.00 ± 6.33	58.33 ± 11.26	0.145*

The data are presented as mean ± standard deviation. * obtained from independent-samples *t*-test, ROM: Range of motion.

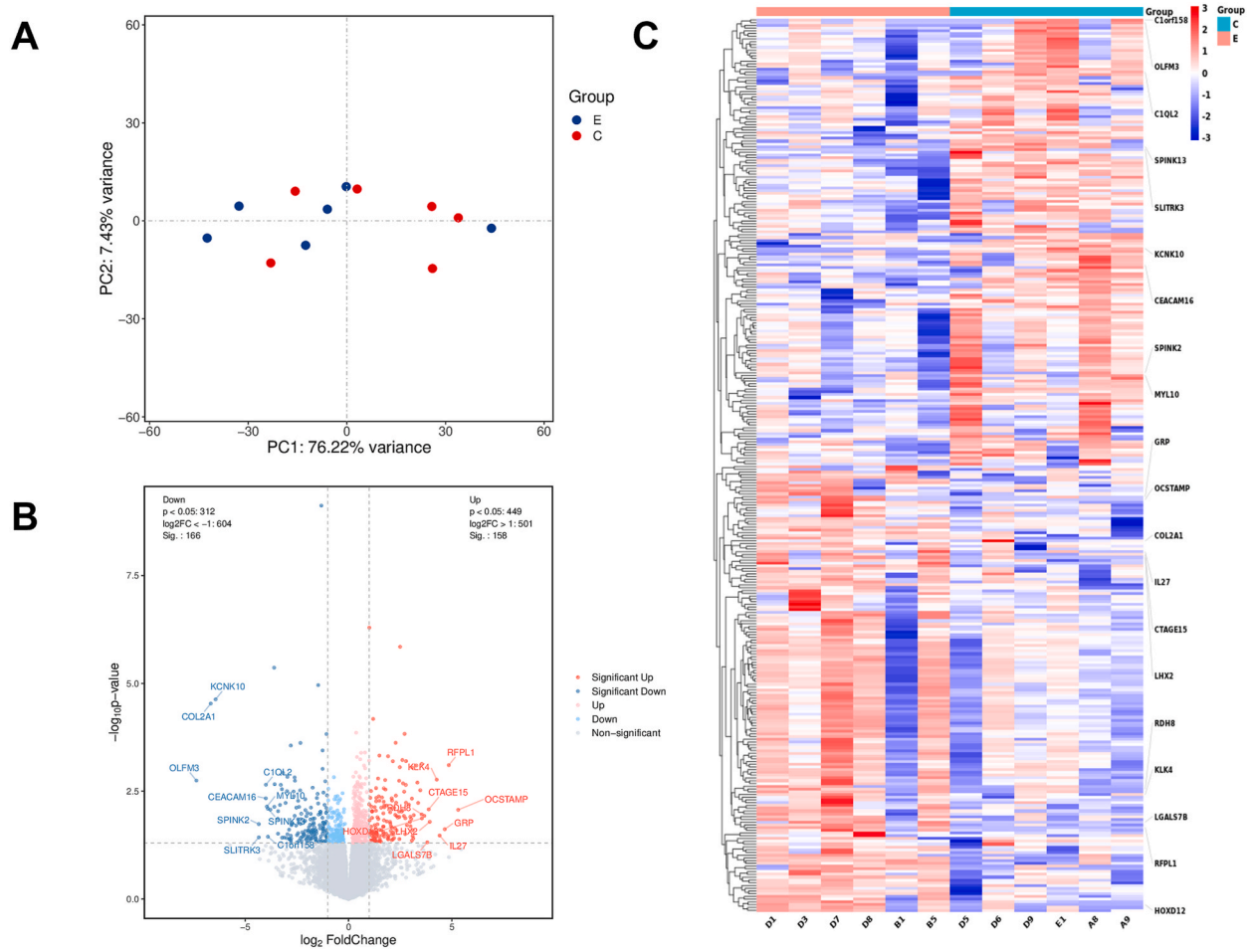

Fig. 1. Principal component analysis (PCA) plot of samples and volcano plot and heat map of the differentially expressed genes (DEGs). (A) PCA plot of samples and (B) Volcano plot of DEGs. The red dots represent upregulated genes and the blue dots represent downregulated genes. The tagged genes are the top 20 genes with a false discovery rate (FDR) < 0.05. (C) Heat map of DEGs.

patients, with or without AC. Table 4 contains the primer sequences used in this experiment. The statistical analysis indicated that the levels of IL6, MMP2, MMP9, COL1A1 and POSTN were notably elevated in the subacromial bursa tissue of RCT patients with AC compared to those without AC. Conversely, MMP1, MMP3, RUNX2, TWIST1 and PTGS2 levels were significantly higher in the tissue samples of RCT patients without AC than in those with AC (Fig. 7).

HE staining and immunohistochemistry results are shown in Fig. 8A,B,C. Significant variations in the staining intensity of MMP2, MMP9 and COL1A1 between the two groups, with no notable differences found in the staining of PTGS2.

4. Discussion

In this study, we screened 324 DEGs and found that 158 of them were upregulated and 166 were downregulated. Following GO enrichment analysis, it was discovered that numerous biological processes associated with the extracellular matrix, such as extracellular matrix disassembly, organization, and collagen catabolic process, were significantly enriched. Additionally, KEGG enrichment analysis indicated significant enrichment of Endocrine resistance, IL-17 signaling pathway, and ECM-receptor interaction. The findings presented indicate a significant involvement of extracellular matrix, metabolic factors, and inflammation in the progression of AC. Then, we identified ten DEGs as hub genes using the STRING database and Cytoscape. We verified the differential expression of these hub genes in two groups of samples by qPCR. Among these DEGs, IL6, MMP2, MMP9, COL1A1, were up-regulated in RCT patients with AC, while MMP1 and MMP3 were down-regulated.

RCT is often accompanied by AC due to several reasons. For example, the pain from the injury can result in reduced joint activity and facilitate the shoulder stiffness. In addition, inflammation caused by RCT can lead to secondary AC [17]. There were many studies about postoperative rehabilitation after RCT [18,19], whose main purposes were to minimize postoperative stiffness incidence and duration. Meanwhile, only a few studies were related to preoperative RCT and concomitant AC. Therefore, we aimed to identify the specific expression genes involved in RCT with AC and we perform functional analysis in order to clarify the molecular pathogenesis of

Table 3
Thirty most strongly upregulated and downregulated genes in RCT patients with AC vs those without AC.

Up-regulated genes in RCT patients with AC compared to RCT patients without AC			
gene_id	description	log2FC	p-value
OCSTAMP	osteoclast stimulatory transmembrane protein	5.3088	0.0085
RFPL1	ret finger protein like 1	4.8538	0.0008
GRP	gastrin releasing peptide	4.6604	0.0241
IL27	interleukin 27	4.4086	0.0337
KLK4	kallikrein related peptidase 4	4.2715	0.0017
LHX2	LIM homeobox 2	3.9347	0.0162
CTAGE15	CTAGE family member 15	3.8828	0.0083
LGALS7B	galectin 7B	3.8139	0.0483
RDH8	retinol dehydrogenase 8	3.6677	0.0118
HOXD12	homeobox D12	3.5525	0.0135
LKAAEAR1	LKAAEAR motif containing 1	3.5455	0.0007
FOSB	FosB proto-oncogene, AP-1 transcription factor subunit	3.4743	0.003
IGSF9	immunoglobulin superfamily member 9	3.3711	0.0059
NKAIN4	sodium/potassium transporting ATPase interacting 4	3.3348	0.002
GABRG1	gamma-aminobutyric acid type A receptor subunit gamma 1	3.2829	0.0008
Down-regulated genes in RCT patients with AC compared to RCT patients without AC			
gene_id	**description**	**log2FC**	**p-value**
OLFM3	olfactomedin 3	−7.3575	0.0018
COL2A1	collagen type II alpha 1 chain	−6.6628	<0.0001
KCNK10	potassium two pore domain channel subfamily K member 10	−6.4295	<0.0001
SPINK2	serine peptidase inhibitor Kazal type 2	−4.3389	0.0183
SLITRK3	SLIT and NTRK like family member 3	−4.3387	0.0371
CEACAM16	CEA cell adhesion molecule 16, tectorial membrane component	−4.0001	0.0046
C1QL2	complement C1q like 2	−3.9972	0.0022
MYL10	myosin light chain 10	−3.9475	0.0072
SPINK13	serine peptidase inhibitor Kazal type 13	−3.9014	0.008
C1orf158	chromosome 1 open reading frame 158	−3.8979	0.0359
PRTN3	proteinase 3	−3.7777	0.0085
CDH22	cadherin 22	−3.5977	<0.0001
TMEM114	transmembrane protein 114	−3.5892	0.0073
MAEL	maelstrom spermatogenic transposon silencer	−3.5737	0.0022
SAA2	serum amyloid A2	−3.421	0.0137

the disease and the strategy of precision medicine.

Matrix Metallopeptidases (MMPs) play a role in breaking down the extracellular matrix during regular physiological functions and tissue restructuring, as well as in conditions like arthritis and tumors. MMPs are also essential for controlling inflammatory responses [20]. Fibroproliferative tissue fibrosis in the shoulder capsule is a key feature of AC, believed to be influenced by cytokines, growth factors, and enzymes like MMPs. There is evidence indicating the involvement of inflammatory mediators and various immune cells in this process [21]. MMP2 and MMP9 gelatinases share motifs resembling fibronectin, which boost their ability to interact with gelatin or gelatin-like substances by assisting in the attachment of fibronectin to denatured collagen [22]. Previous studies have shown that MMP2 and MMP9 upregulate in the development of AC, both in tissues collected from human patients and the rat contracture model [23,24]. MMP2 and MMP9 have been discovered to involve in the survival, growth, movement, and infiltration of synovial fibroblasts in rheumatoid arthritis, a different chronic inflammatory condition [25]. Synovial fibroblasts have been suggested to potentially accelerate the development of pathological fibrosis in FS [26], possibly through activation and production of inflammatory cytokines [27]. MMP2 is also involved in the degradation of the proteoglycan Decorin, which induces the release of transforming growth factor beta (TGFβ) [28]. Fibroblasts are significantly influenced by TGF-β, which is essential in the development of fibrosis [29]. In addition to MMP2 and MMP9, other MMPs (such as MMP11, MMP13, MMP14 and MMP17) are also identified as DEGs. They are likely to participate in the fibrosis process of AC. MMP1, MMP3, MMP9, MMP13 and IL6 are also involved in IL-17 signaling pathway. These findings indicate that the MMPs family plays a significant part in the occurrence of AC.

The IL6 gene produces a protein that involves in the immune response to inflammation. This interleukin involves in numerous disease conditions related to inflammation, such as diabetes mellitus [30] and rheumatoid arthritis [31]. IL6 is upregulated in AC synovial fibroblasts and promotes AC fibrosis through the PI3K-Akt signaling pathway [32]. It had also been detected in subacromial bursa and synovial tissues of AC patients [33,34]. Genes related to inflammatory response, such as CCL16, IL27, NLRP6, PTGS2, were screened as DEGs. IL27 and IL6 belong to the IL6 family and both utilize the shared signaling receptor subunit glycoprotein 130 kDa (gp130) [35]. IL6 and IL27 regulate the signal transducer and activator of transcription 1 (STAT1) and STAT3 signaling pathways to affect the effector properties of T cells. IL27 inhibits the differentiation of Th17 cells by enhancing STAT1 activity [36]. Recent research has shown that patients with AC have a high concentration of T cells in the shoulder capsule tissue. $CD4^+$ CD127+ T cells expressed Th17 related genes [37]. The upregulation of IL27 expression that we found may be an attempt by the body to regulate the inflammatory response, thereby maintaining immune balance and controlling inflammation. IL6 activates the JAK-STAT signaling pathway to increase PTGS2 expression [38]. In turn, PTGS2 products, particularly Prostaglandin E2 (PGE2), can increase IL6

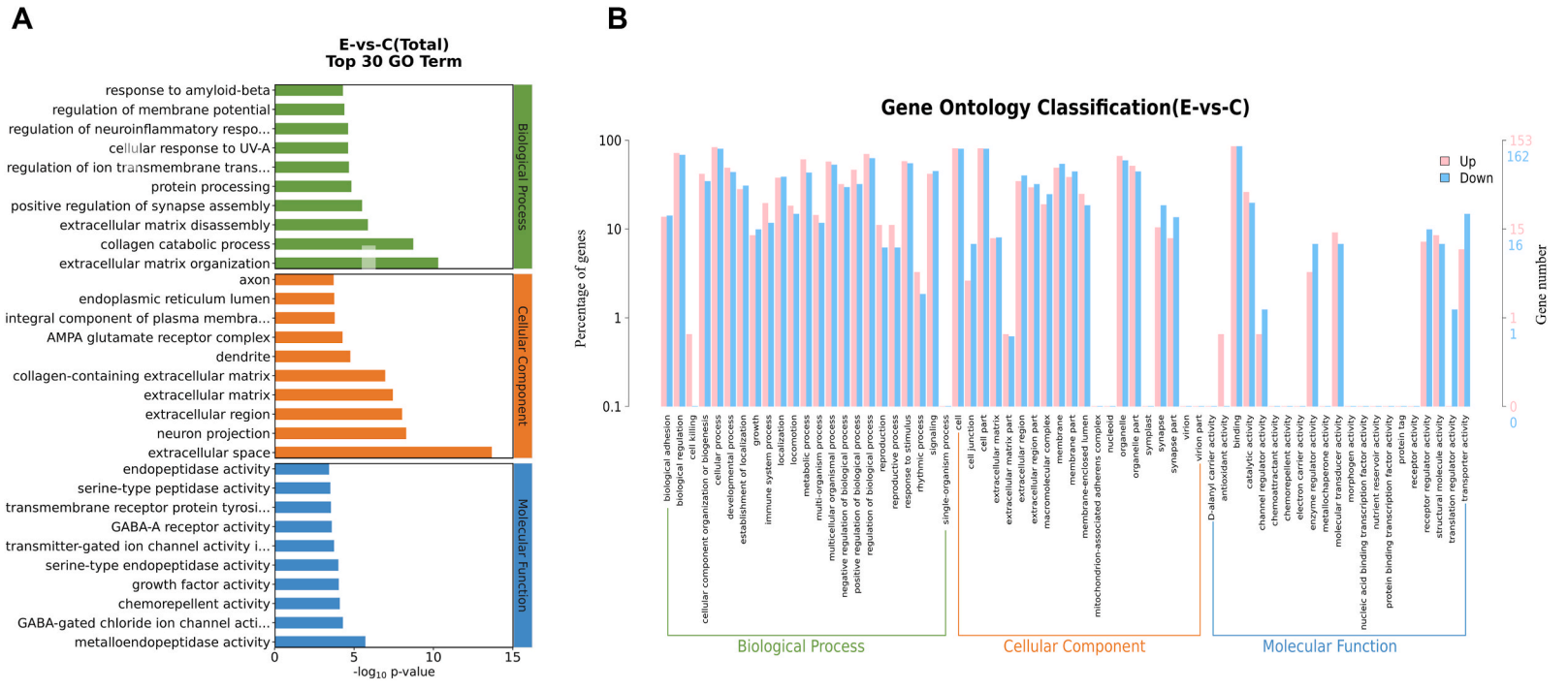

Fig. 2. GO analysis. (A) Bar Chart of the GO functional enrichment analysis (the top 10 terms of each domain). (B) Pink represents GO Level2 entries with up regulation of DEGs, light blue represents GO Level2 entries with down regulation of DEGs.

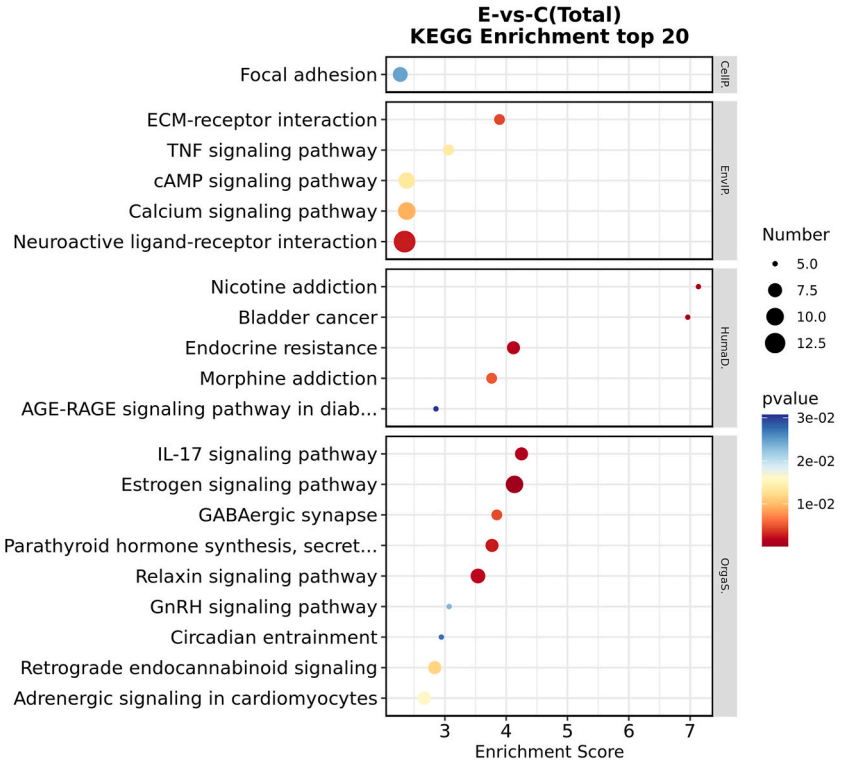

Fig. 3. The kyoto encyclopedia of genes and genomes (KEGG) pathway analysis.

expression [39]. These genes suggest that AC is an inflammatory condition.

The shoulder joint capsule, which is in good health, is made up of dense type I collagen and elastic fiber bundles, giving it a collagenous structure. Fibroblasts support the capsule integrity by generating proteins in the extracellular matrix (ECM) that offer a strong yet adaptable framework. KEGG pathway analysis showed the genes COL1A1, COL2A1, COL4A4, COL28A1 encoding collagen participate in the above process through ECM-receptor interaction.

The primary innovation of this study is the unique grouping of patients with RCT based on the presence or absence of AC, and the utilization of transcriptome sequencing analysis of subacromial bursa samples from each group. Previous studies have focused on the differences in the transcriptome of tendons in RCT patients based on tear etiology and gender [40]. In contrast, by comparing the molecular differences between adhesive and non-adhesive patients, we provide fresh perspectives on the pathogenesis of AC, especially in the molecular processes involved in adhesion formation. Prior research has utilized PCR to evaluate the gene expression of inflammatory and fibrosis-related factors in individuals with AC and RCT [2]. Our study used transcriptome sequencing technology, which is a more comprehensive and high-throughput analysis. Transcriptome sequencing allows us to go beyond the analysis of preselected genes to reveal unknown or unanticipated bioinformatics findings. The application of this method provides unprecedented detail and depth for comparing RCT patients with and without AC. By systematically analyzing and comparing transcriptome data, distinct gene expression signatures between two clinically relevant patient subgroups were established, and potential biomarkers were identified. In the future, this may provide stronger scientific support for the treatment decisions of patients with RCT, and provide guidance for future clinical interventions.

Although our study has made certain findings and progress, it is important to consider several limitations when discussing our results. Firstly, we did not use Western blotting to verify the protein expression results, instead, we used immunohistochemistry to validate our findings at the protein level. Secondly, the study had a small sample size, potentially restricting the applicability of our results. To validate these findings, it would be useful to expand the sample size in future studies. Additionally, our preliminary results are promising, but they need to be validated in a wider range of samples and by using multiple methods, including Western blotting. We encourage future work to utilize these techniques and expand the sample size to further investigate and confirm our findings.

5. Conclusion

In summary, this study investigated the transcriptome of RCT accompanied with AC, and compared with the simple RCT without AC. Bioinformatics was used to identify DEGs and analyze their KEGG pathway enrichment and GO functional enrichment. MMP1, MMP2, MMP3, MMP9, IL6, COL1A1 and POSTN were screened as hub DEGs and verified by qPCR. The research expanded the data on gene expression profiles of DEGs in the subacromial bursa tissue of RCT patients, with or without AC, offering fresh perspectives on

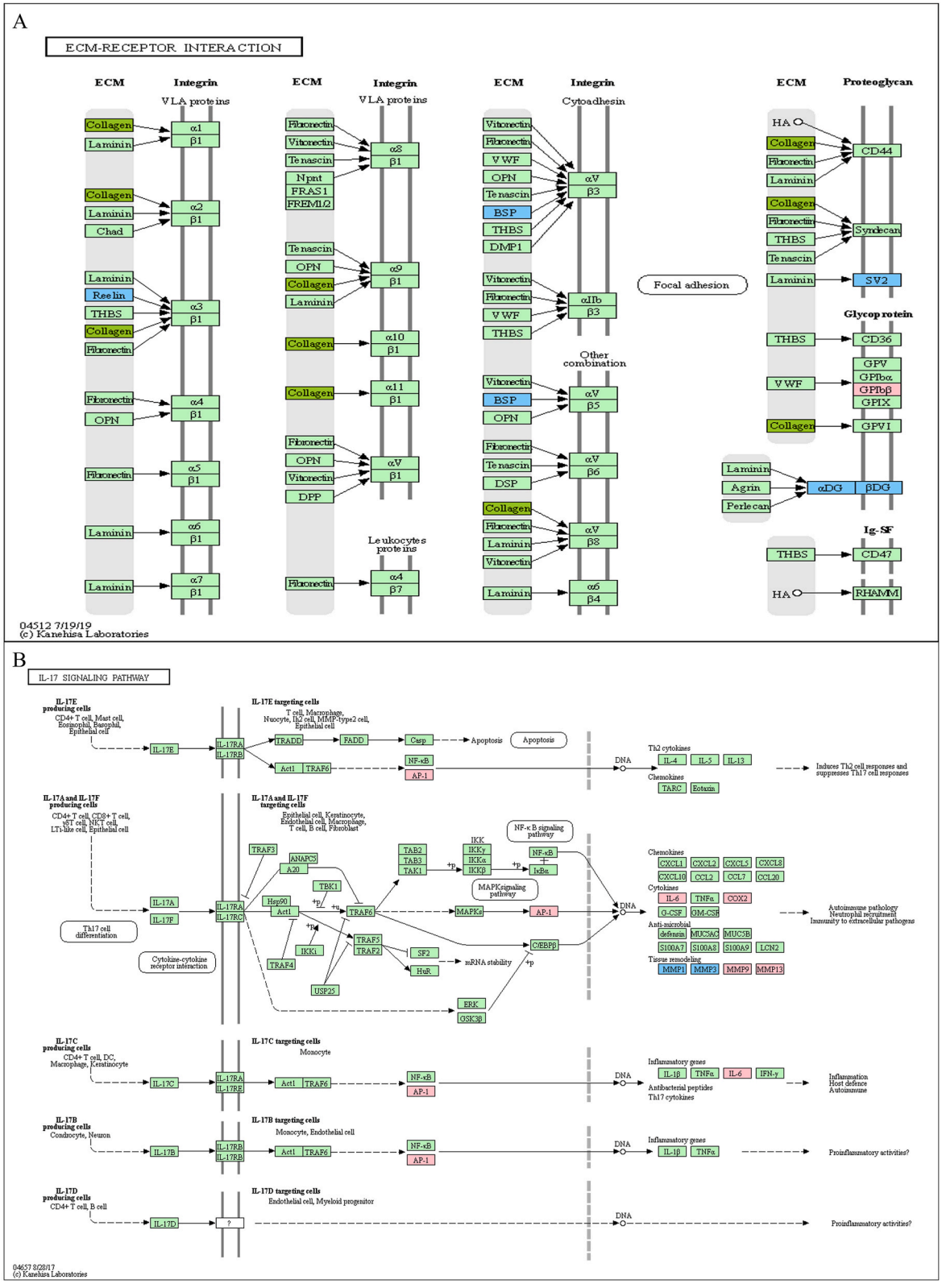

Fig. 4. (A) The ECM-receptor interaction pathway and (B) the IL-17 signaling pathway. The red boxes represent upregulated genes and the light blue boxes represent downregulated genes. (For interpretation of the references to colour in this figure legend, the reader is referred to the Web version of this article.)

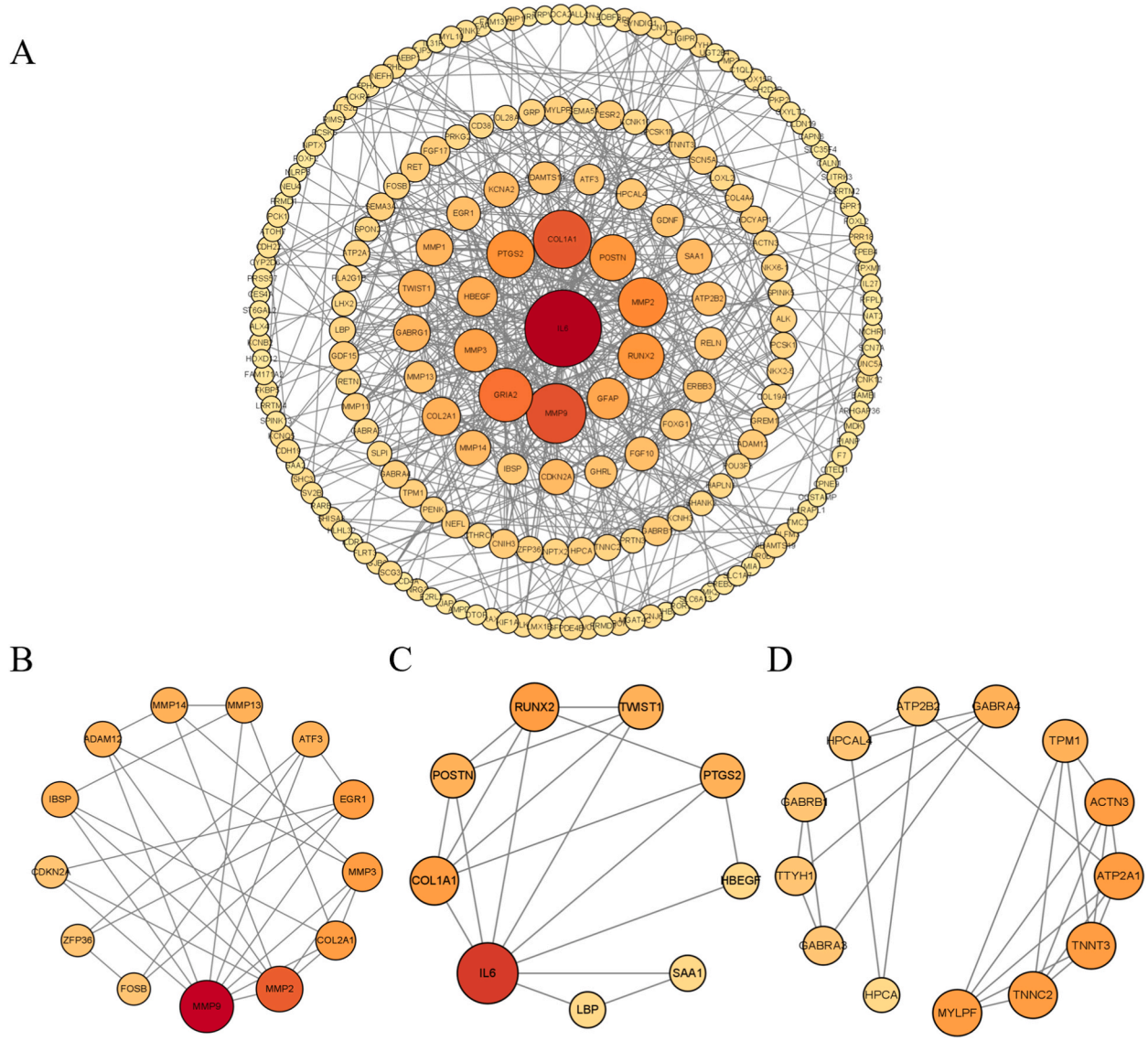

Fig. 5. The PPI network (A) and hub genes (top three modules). (B,C,D) The significant modules identified by the Molecular Complex Detection (MCODE) and the cytoHubba plugin of Cytoscape.

gene expression transcriptional regulation. Additional mechanistic research is required to ascertain the importance of these variances in the development of the illness.

Ethics statement

This study was performed in agreement with the Declaration of Helsinki, and with local and national laws. This work was approved by the clinical research ethics committee at the First Affiliated Hospital of Soochow University (2022–007), and all participants signed an informed written consent before inclusion in the study.

Consent for publication

Not applicable.

Data availability statement

The transcriptome sequencing data generated in this study have been deposited in the NCBI Sequence Read Archive (SRA). The data

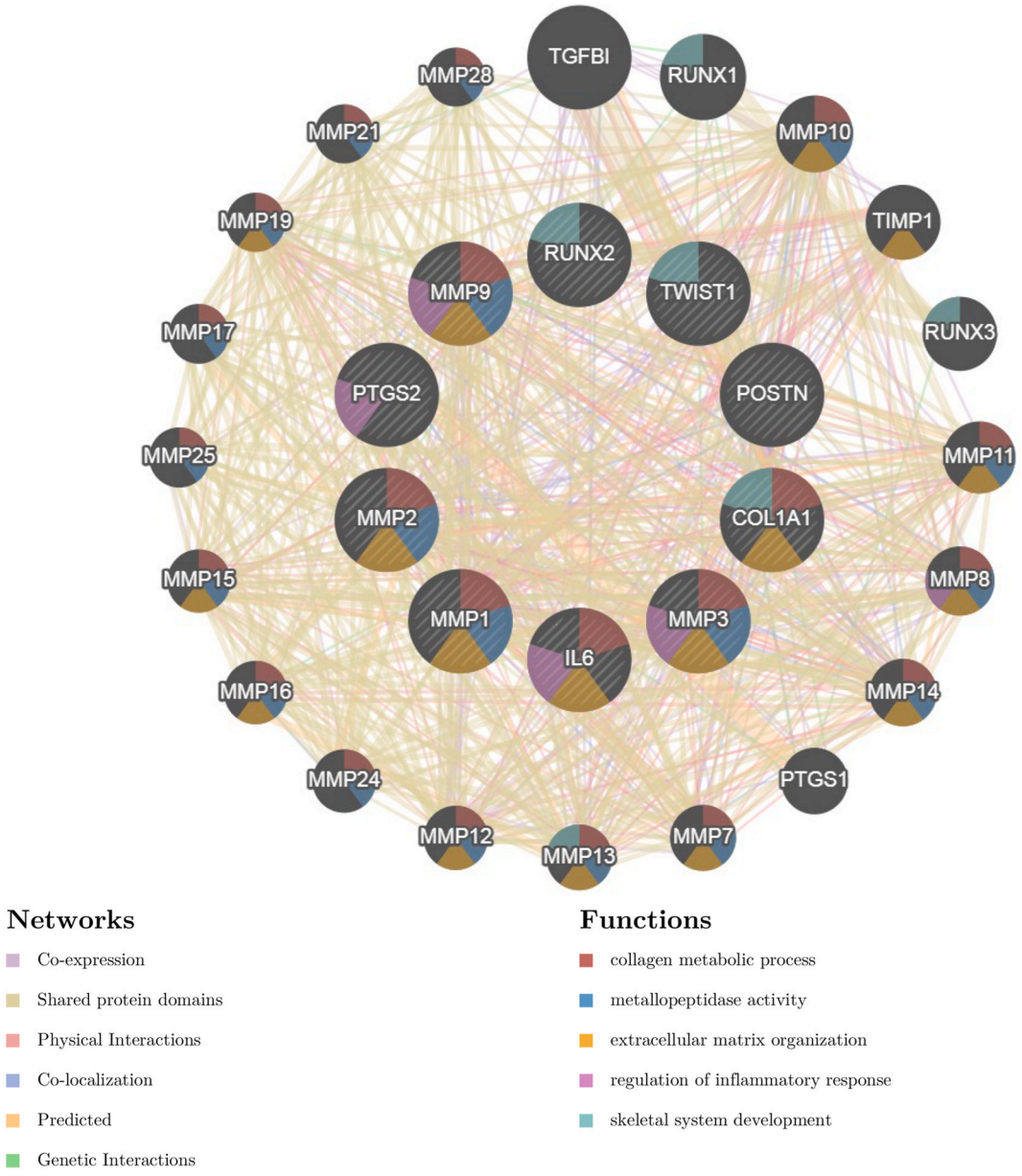

Fig. 6. Hub genes and their co-expression genes were analyzed via GeneMANIA.

are accessible through the SRA accession number [PRJNA1082194]. This dataset includes raw sequencing reads for all samples analyzed in this study. The data underpin the findings presented herein and can be freely accessed by researchers in accordance with the terms and conditions of the SRA database. The other datasets used and analyzed during the study available from the corresponding author on reasonable request.

Funding

This work was supported by National Key Research and Development Program of China (grant number 2022YFE0199900), Clinical Application-oriented Medical Innovation Foundation (grant number 2021-NCRC-CXJJ-PY-09) from National Clinical Research Center for Orthopedics, Sports Medicine & Rehabilitation and Jiangsu China-Israel Industrial Technical Research Institute Foundation, Jiangsu Province Science and Technology Innovation Support Plan Project (grant number BZ2022051), China-Europe Sports Medicine Belt-and-Road Joint Laboratory, Ministry of Education of PRC (grant number 2023297), and Key Research Project of Higher Education Teaching Reform of Soochow University (grant number 2023–12).

Role of the Funder/Sponsor: The funders had no role in the design and conduct of the study; collection, management, analysis, and

Table 4
Gene primer sequences.

Gene	Primer sequence	
IL6	Forward	5′-ATGAGGAGACTTGCCTGGTGAA-3′
	Reverse	5′CTCTGGCTTGTTCCTCACTACTCTC-3′
MMP1	Forward	5′-GACCTACAGGATTGAAAATTACACG-3′
	Reverse	5′-GCAAGATTTCCTCCAGGTCCAT-3′
MMP2	Forward	5′-TGTTGGTGGGAACTCAGAAGGT-3′
	Reverse	5′-GACGGAAGTTCTTGGTGTAGGTGT-3′
MMP3	Forward	5′-GAGGACACCAGCATGAACCTTG-3′
	Reverse	5′-CAATCCTGTATGTAAGGTGGGT-3′
MMP9	Forward	5′-GAAGATGCTGCTGTTCAGCG-3′
	Reverse	5′-GGTCCTGGCAGAAATAGGCTT-3′
COL1A1	Forward	5′-TGGCAAAGATGGACTCAACG-3′
	Reverse	5′-TCACGGTCACGAACCACATT-3′
POSTN	Forward	5′-TTGGCTCATAGTCGTATCAGGG-3′
	Reverse	5′-GCAGCCTTTCATTCCTTCCAT-3′
RUNX2	Forward	5′-CTACTATGGCACTTCGTCAGGAT-3′
	Reverse	5′-ATCAGCGTCAACACCATCATT-3′
TWIST1	Forward	5′-CTCGGACAAGCTGAGCAAGA-3′
	Reverse	5′-CTCCATCCTCCAGACCGAGA-3′
PTGS2	Forward	5′-GGGTTGCTGGTGGTAGGAATG-3′
	Reverse	5′-CATAAAGCGTTTGCGGTACTCAT-3′
GAPDH	Forward	5′-GGAAGCTTGTCATCAATGGAAATC-3′
	Reverse	5′-TGATGACCCTTTTGGCTCCC-3′

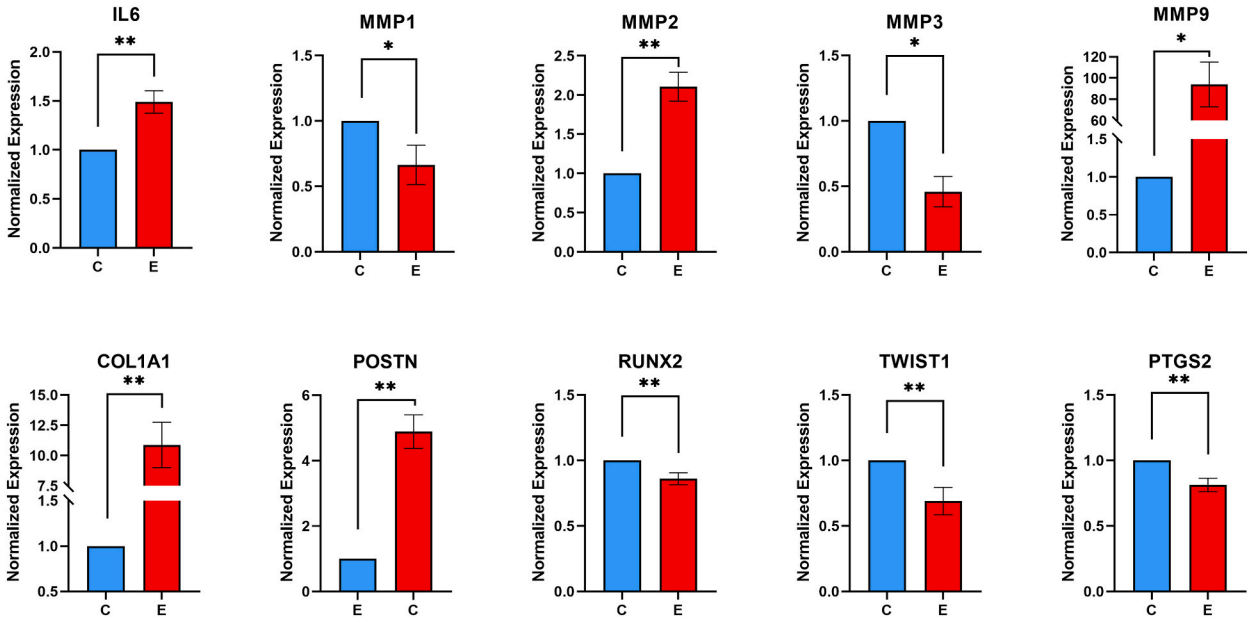

Fig. 7. Validation of expression of selected transcripts by real-time qPCR. *p < 0.05, **p < 0.01.

interpretation of the data; preparation, review, or approval of the manuscript; and decision to submit the manuscript for publication.

Availability of data and materials

The datasets generated during and/or analyzed during the current study are available from the corresponding author on reasonable request.

CRediT authorship contribution statement

Qiuyuan Wang: Writing – review & editing, Writing – original draft, Formal analysis, Data curation. **Feng Zhou:** Writing – original draft, Conceptualization. **Pingcheng Xu:** Formal analysis, Data curation. **Lingying Zhao:** Supervision, Methodology, Funding acquisition, Conceptualization. **Jiong Jiong Guo:** Writing – review & editing, Supervision, Investigation, Funding acquisition, Data

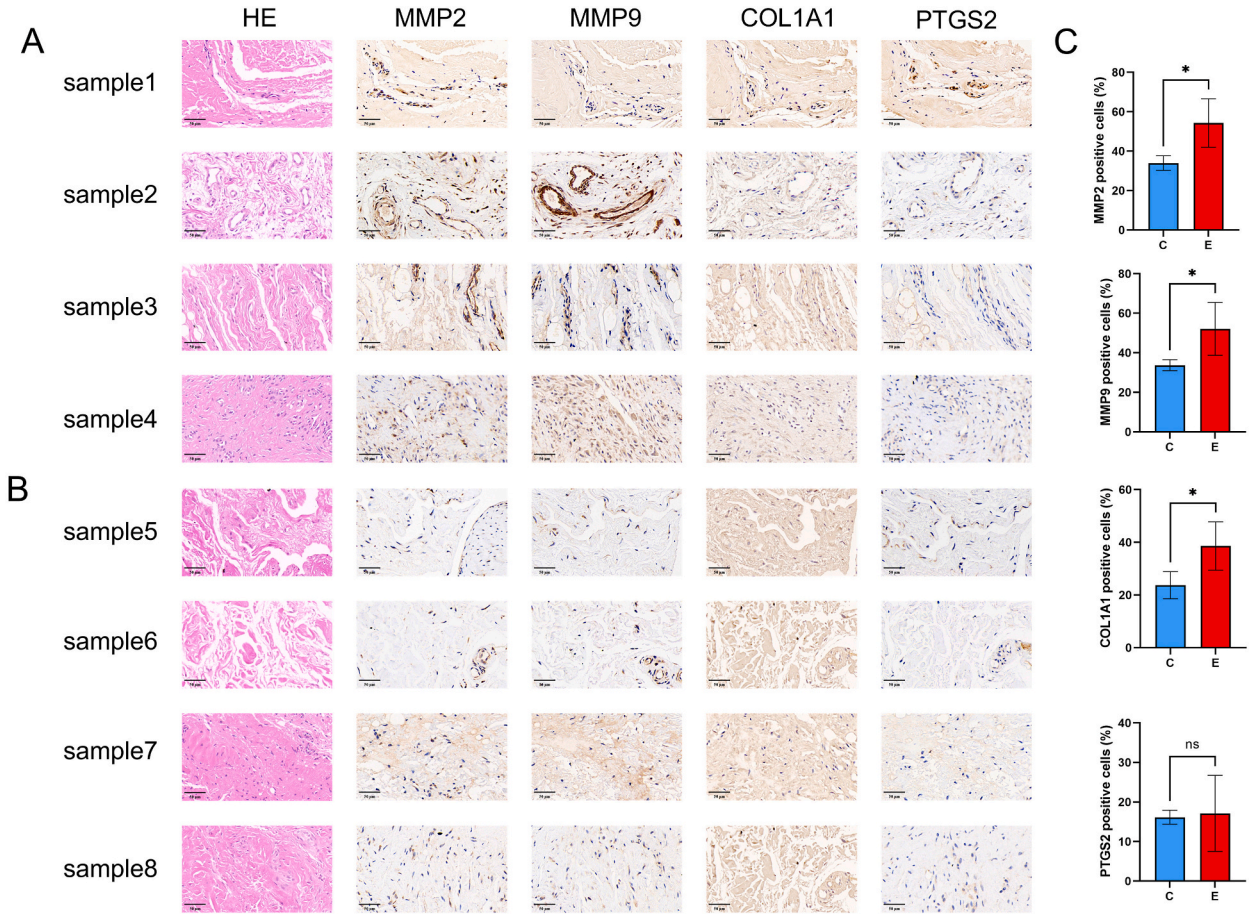

Fig. 8. (A) Immunohistochemical analysis of samples from RCT patients with AC. (B) Immunohistochemical analysis of samples from RCT patients without AC. (C) Quantitative analysis of the percentage of positive cells. Scar bar is 50 μm *p < 0.05, NS not significant.

curation, Conceptualization.

Declaration of competing interest

The authors declare the following financial interests/personal relationships which may be considered as potential competing interests: Jiong Jiong Guo reports financial support was provided by National Key Research and Development Program of China. Jiong Jiong Guo reports financial support was provided by Jiangsu Province Science and Technology Innovation Support Plan Project. Jiong Jiong Guo reports financial support was provided by China-Europe Sports Medicine Belt-and-Road Joint Laboratory, Ministry of Education of PRC. Jiong Jiong Guo reports financial support was provided by Key Research Project of Higher Education Teaching Reform of Soochow University. If there are other authors, they declare that they have no known competing financial interests or personal relationships that could have appeared to influence the work reported in this paper.

Acknowledgements

We dedicate this article to the memories of Ms Lingfen Zhou, the mother of Dr. JJ Guo, who made important contributions to the development and realization of this project.

Abbreviations

AC	Adhesive capsulitis
BP	Biological process
CC	Cellular component
CCL16	C–C motif chemokine ligand 16
COL1A1	Collagen Type I Alpha 1 Chain

COL28A1 Collagen type XXVIII alpha 1 chain
COL2A1 Collagen type II alpha 1 chain
COL4A4 Collagen type IV alpha 4 chain
DEGs Differentially expressed genes
ECM Extracellular matrix
FPKM Fragments Per Kilobase of exon model per Million mapped fragments
GAPDH Glyceraldehyde-3-phosphate dehydrogenase
GO Gene Ontology
gp130 glycoprotein 130 kDa
HE Hematoxylin-eosin
IHC Immunohistochemistry
IL6 Interleukin 6
IL17 Interleukin 17
IL27 Interleukin 27
IRS immunoreaction score
KEGG Kyoto Encyclopedia of Genes and Genomes
MCODE Molecular Complex Detection
MF Molecular function
MMP1 Matrix Metallopeptidase 1
MMP2 Matrix Metallopeptidase 2
MMP3 Matrix Metallopeptidase 3
MMP9 Matrix Metallopeptidase 9
MMP11 Matrix Metallopeptidase 11
MMP13 Matrix Metallopeptidase 13
MMP14 Matrix Metallopeptidase 14
MMP17 Matrix Metallopeptidase 17
NLRP6 NLR family pyrin domain containing 6
PCA Principal component analysis
PGE2 Prostaglandin E2
POSTN Periostin
PPI Protein-protein interaction
PTGS2 Prostaglandin-Endoperoxide Synthase 2
qRT-PCR Real-time Quantitative polymerase chain reaction
RCT Rotator cuff tear
ROM Range of motion
RUNX2 RUNX Family Transcription Factor 2
STAT1 signal transducer and activator of transcription 1
STAT3 signal transducer and activator of transcription 3
STRING Search Tool for the Retrieval of Interacting Genes/Proteins
TWIST1 Twist Family BHLH Transcription Factor 1

Appendix A. Supplementary data

Supplementary data to this article can be found online at https://doi.org/10.1016/j.heliyon.2024.e30512.

References

[1] R.Z. Tashjian, Epidemiology, natural history, and indications for treatment of rotator cuff tears, Clin. Sports Med. 31 (4) (2012) 589–604.
[2] Y.S. Kim, Y.G. Lee, H.S. Park, R.K. Cho, H.J. Lee, Comparison of gene expression of inflammation- and fibrosis-related factors between the anterior and posterior capsule in patients with rotator cuff tear and shoulder stiffness, Orthop J Sports Med 9 (10) (2021) 23259671211032543.
[3] N. Shah, M. Lewis, Shoulder adhesive capsulitis: systematic review of randomised trials using multiple corticosteroid injections, Br. J. Gen. Pract. 57 (541) (2007) 662–667.
[4] C.H. Cho, K.C. Bae, D.H. Kim, Treatment strategy for frozen shoulder, Clin. Orthop. Surg. 11 (3) (2019) 249–257.
[5] H.S. Park, K.H. Choi, H.J. Lee, Y.S. Kim, Rotator cuff tear with joint stiffness: a review of current treatment and rehabilitation, Clin Shoulder Elb 23 (2) (2020) 109–117.
[6] G. Deprés-Tremblay, A. Chevrier, M. Snow, M.B. Hurtig, S. Rodeo, M.D. Buschmann, Rotator cuff repair: a review of surgical techniques, animal models, and new technologies under development, J. Shoulder Elbow Surg. 25 (12) (2016) 2078–2085.
[7] Y. Sun, S. Liu, S. Chen, J. Chen, The effect of corticosteroid injection into rotator interval for early frozen shoulder: a randomized controlled trial, Am. J. Sports Med. 46 (3) (2018) 663–670.
[8] S. Chen, Y. Zhou, Y. Chen, J. Gu, fastp: an ultra-fast all-in-one FASTQ preprocessor, Bioinformatics 34 (17) (2018) i884–i890.
[9] D. Kim, B. Langmead, S.L. Salzberg, HISAT: a fast spliced aligner with low memory requirements, Nat. Methods 12 (4) (2015) 357–360.

[10] A. Roberts, C. Trapnell, J. Donaghey, J.L. Rinn, L. Pachter, Improving RNA-Seq expression estimates by correcting for fragment bias, Genome Biol. 12 (3) (2011) R22.
[11] S. Anders, P.T. Pyl, W. Huber, HTSeq–a Python framework to work with high-throughput sequencing data, Bioinformatics 31 (2) (2015) 166–169.
[12] M.I. Love, W. Huber, S. Anders, Moderated estimation of fold change and dispersion for RNA-seq data with DESeq2, Genome Biol. 15 (12) (2014) 550.
[13] The gene Ontology resource: 20 years and still GOing strong, Nucleic Acids Res. 47 (D1) (2019) D330–d338.
[14] M. Kanehisa, M. Araki, S. Goto, M. Hattori, M. Hirakawa, M. Itoh, T. Katayama, S. Kawashima, S. Okuda, T. Tokimatsu, et al., KEGG for linking genomes to life and the environment, Nucleic Acids Res. 36 (Database issue) (2008) D480–D484.
[15] D. Szklarczyk, A. Franceschini, S. Wyder, K. Forslund, D. Heller, J. Huerta-Cepas, M. Simonovic, A. Roth, A. Santos, K.P. Tsafou, et al., STRING v10: protein-protein interaction networks, integrated over the tree of life, Nucleic Acids Res. 43 (Database issue) (2015) D447–D452.
[16] D. Warde-Farley, S.L. Donaldson, O. Comes, K. Zuberi, R. Badrawi, P. Chao, M. Franz, C. Grouios, F. Kazi, C.T. Lopes, et al., The GeneMANIA prediction server: biological network integration for gene prioritization and predicting gene function, Nucleic Acids Res. 38 (Web Server issue) (2010) W214–W220.
[17] J.C. Tauro, Stiffness and rotator cuff tears: incidence, arthroscopic findings, and treatment results, Arthroscopy 22 (6) (2006) 581–586.
[18] C.A. Thigpen, M.A. Shaffer, B.W. Gaunt, B.G. Leggin, G.R. Williams, R.B. Wilcox, 3rd: the American Society of Shoulder and Elbow Therapists' consensus statement on rehabilitation following arthroscopic rotator cuff repair, J. Shoulder Elbow Surg. 25 (4) (2016) 521–535.
[19] J.D. Keener, L.M. Galatz, G. Stobbs-Cucchi, R. Patton, K. Yamaguchi, Rehabilitation following arthroscopic rotator cuff repair: a prospective randomized trial of immobilization compared with early motion, J Bone Joint Surg Am 96 (1) (2014) 11–19.
[20] K. Kessenbrock, V. Plaks, Z. Werb, Matrix metalloproteinases: regulators of the tumor microenvironment, Cell 141 (1) (2010) 52–67.
[21] N.L. Millar, A. Meakins, F. Struyf, E. Willmore, A.L. Campbell, P.D. Kirwan, M. Akbar, L. Moore, J.C. Ronquillo, G.A.C. Murrell, et al., Frozen shoulder, Nat. Rev. Dis. Prim. 8 (1) (2022) 59.
[22] W.C. Parks, C.L. Wilson, Y.S. López-Boado, Matrix metalloproteinases as modulators of inflammation and innate immunity, Nat. Rev. Immunol. 4 (8) (2004) 617–629.
[23] L. Marker, P. Schjerling, A.L. Mackey, T. Hansen, J. Jakobsen, M. Kjær, M.R. Krogsgaard, Collagens in primary frozen shoulder: expression of collagen mRNA isoforms in the different phases of the disease, Rheumatology 60 (8) (2021) 3879–3887.
[24] C.H. Cho, Y.M. Lho, I. Hwang, D.H. Kim, Role of matrix metalloproteinases 2 and 9 in the development of frozen shoulder: human data and experimental analysis in a rat contracture model, J. Shoulder Elbow Surg. 28 (7) (2019) 1265–1272.
[25] M. Xue, K. McKelvey, K. Shen, N. Minhas, L. March, S.Y. Park, C.J. Jackson, Endogenous MMP-9 and not MMP-2 promotes rheumatoid synovial fibroblast survival, inflammation and cartilage degradation, Rheumatology 53 (12) (2014) 2270–2279.
[26] C.M. Hettrich, E.F. DiCarlo, D. Faryniarz, K.B. Vadasdi, R. Williams, J.A. Hannafin, The effect of myofibroblasts and corticosteroid injections in adhesive capsulitis, J. Shoulder Elbow Surg. 25 (8) (2016) 1274–1279.
[27] M. Akbar, M. McLean, E. Garcia-Melchor, L.A. Crowe, P. McMillan, U.G. Fazzi, D. Martin, A. Arthur, J.H. Reilly, I.B. McInnes, et al., Fibroblast activation and inflammation in frozen shoulder, PLoS One 14 (4) (2019) e0215301.
[28] K. Imai, A. Hiramatsu, D. Fukushima, M.D. Pierschbacher, Y. Okada, Degradation of decorin by matrix metalloproteinases: identification of the cleavage sites, kinetic analyses and transforming growth factor-beta 1 release, Biochem. J. 322 (Pt 3) (1997) 809–814. Pt 3.
[29] N. Frangogiannis, Transforming growth factor-β in tissue fibrosis, J. Exp. Med. 217 (3) (2020) e20190103.
[30] P.J. White, P. St-Pierre, A. Charbonneau, P.L. Mitchell, E. St-Amand, B. Marcotte, A. Marette, Protectin DX alleviates insulin resistance by activating a myokine-liver glucoregulatory axis, Nat. Med. 20 (6) (2014) 664–669.
[31] F. Zhang, K. Wei, K. Slowikowski, C.Y. Fonseka, D.A. Rao, S. Kelly, S.M. Goodman, D. Tabechian, L.B. Hughes, K. Salomon-Escoto, et al., Defining inflammatory cell states in rheumatoid arthritis joint synovial tissues by integrating single-cell transcriptomics and mass cytometry, Nat. Immunol. 20 (7) (2019) 928–942.
[32] R. Yang, Y. Tang, J. Hou, M. Yu, Y. Long, A. Yamuhanmode, Q. Li, F. Li, Y. Zhang, M. Warsame, et al., Fibrosis in frozen shoulder: activation of IL-6 through PI3K-Akt signaling pathway in synovial fibroblast, Mol. Immunol. 150 (2022) 29–38.
[33] H. Nishimoto, S. Fukuta, N. Fukui, K. Sairyo, T. Yamaguchi, Characteristics of gene expression in frozen shoulder, BMC Muscoskel. Disord. 23 (1) (2022) 811.
[34] J. Cui, T. Zhang, J. Xiong, W. Lu, L. Duan, W. Zhu, D. Wang, RNA-sequence analysis of samples from patients with idiopathic adhesive capsulitis, Mol. Med. Rep. 16 (5) (2017) 7665–7672.
[35] S. Rose-John, Interleukin-6 family cytokines, Cold Spring Harbor Perspect. Biol. 10 (2) (2018).
[36] S.A. Jones, B.J. Jenkins, Recent insights into targeting the IL-6 cytokine family in inflammatory diseases and cancer, Nat. Rev. Immunol. 18 (12) (2018) 773–789.
[37] M.T.H. Ng, R. Borst, H. Gacaferi, S. Davidson, J.E. Ackerman, P.A. Johnson, C.C. Machado, I. Reekie, M. Attar, D. Windell, et al., A single cell atlas of frozen shoulder capsule identifies features associated with inflammatory fibrosis resolution, Nat. Commun. 15 (1) (2024) 1394.
[38] B. Dawn, Y.T. Xuan, Y. Guo, A. Rezazadeh, A.B. Stein, G. Hunt, W.J. Wu, W. Tan, R. Bolli, IL-6 plays an obligatory role in late preconditioning via JAK-STAT signaling and upregulation of iNOS and COX-2, Cardiovasc. Res. 64 (1) (2004) 61–71.
[39] H. Inoue, M. Takamori, Y. Shimoyama, H. Ishibashi, S. Yamamoto, Y. Koshihara, Regulation by PGE2 of the production of interleukin-6, macrophage colony stimulating factor, and vascular endothelial growth factor in human synovial fibroblasts, Br. J. Pharmacol. 136 (2) (2002) 287–295.
[40] M.F. Rai, L. Cai, E.D. Tycksen, J. Keener, A. Chamberlain, RNA-Seq reveals distinct transcriptomic differences in rotator cuff tendon based on tear etiology and patient sex, J. Orthop. Res. 40 (12) (2022) 2728–2742.